Biochimica et Biophysica Acta, 1027 (1990) 8–16
Elsevier

BBAMEM 74921

The Na^+-dependent proline carrier, of eel intestinal brush-border membrane, sequentially binds proline and then Na^+

Michele Maffia, Giuseppe Cassano, Daniela Marcucci, Sebastiano Vilella and Carlo Storelli

Laboratorio di Fisiologia, Università di Lecce, Lecce (Italy)

(Received 1 November 1989)
(Revised manuscript received 17 April 1990)

Key words: Brush-border membrane; Sodium ion cotransport; Proline; Amino acid transport; Intestinal transport; (*A. anguilla*)

The mechanism of Na^+/L-proline cotransport, present on brush-border membrane (BBM) vesicles of the European eel intestine, was studied. Initial cotransport rates, depending on increasing proline and Na^+ concentrations in the extravesicular medium (zero-trans conditions), were measured by monitoring the decay of an inside-negative membrane potential, i.e. the fluorescence quenching of the voltage-sensitive cyanine dye 3,3′-diethylthiacarbocyanine iodide (DiS-C_2(5)). By simultaneously estimating the substrate-dependent Na^+-influx (with the fluorescent dye) and the Na^+-dependent [^{3}H]substrate influx, it was concluded that proline was cotransported with 1 Na^+ ion and glucose with 2 Na^+ ions. The kinetics of proline/Na^+ cotransport were then investigated. Graphical analysis excluded a ping-pong mechanism. Under rapid equilibrium assumptions, by fitting model equations to rate values it was possible to exclude the random and the ordered Na^+/proline mechanisms. Therefore, in eel intestinal BBM vesicles, the mechanism of proline/Na^+ cotransport is ordered and $proline_{out}$ binds to the carrier prior to Na^+_{out}.

Introduction

In the intestinal brush-border membrane (BBM), the uphill amino acid translocation is coupled to the downhill Na^+ influx [1]; moreover Na^+-independent carriers have been also characterized [2–4] for all amino acids with the exception of proline, at least in BBM of the eel intestine [5].

Studies with BBM vesicles from rabbit intestine showed that proline/Na^+ cotransport occurs mainly via an agency specific for prolines and N-methylated amino acids and therefore called IMINO system [6,7]. The Na^+/proline cotransporter present on BBM of the eel intestine revealed some differences from the rabbit IMINO system: (a) Na^+-dependent proline uptake was totally (and not partially) inhibited by alanine and partially (and not totally) inhibited by phenylalanine; (b) Hill analysis, under short-circuited membrane potential conditions, indicated n (Hill index) = 1 in the eel and 2 in the rabbit [5,8].

Correspondence: M. Maffia, Laboratorio di Fisiologia, Dipartimento di Biologia, Università di Lecce, Strada Prov. le Monteroni, 73100 Lecce, Italy.

To further characterize the proline/Na^+ cotransporter present on BBM of the eel intestine, we carried out a kinetic analysis of the initial out > in rates in the presence of inside-negative membrane potential. The proline-dependent Na^+ influx was monitored by recording the fluorescence quenching of the voltage-sensitive dye diS-$_2$(5) [9].

Materials and Methods

Materials

European yellow eels (*Anguilla anguilla*) (150–200 g) were purchased from a commercial source (Ittica Ugento, Lecce, Italy) and maintained in sea water aquariums. All chemicals, reagent grade, were obtained from Merck (Darmstadt, F.R.G.) valinomycin from Sigma (St. Louis, MO) and 3,3′-diethylthiadicarbocyanine iodine (DiS-C_2(5)) from Eastman Kodak (Rochester, NY). D-[^{3}H]Glucose and L-[^{3}H]proline were obtained from New England Nuclear (Boston, MA).

Preparation of brush-border membrane vesicles

Brush-border membrane (BBM) vesicles were prepared from the intestine of yellow eels, as described elsewhere [10]; the preparation method is based on selective precipitation of all cellular component, with

the exception of BBM, in the presence of ethyleneglycol bis(β-aminoethyl ether)-*N*,*N*'-tetraacetic acid (EGTA) and 12 mM $MgCl_2$. BBM fractions routinely showed enrichment factors over the initial homogenate of at least 16 for leucine aminopeptidase, 12 for maltase and 13 for alkaline phosphatase; no enrichment was found for marker enzymes of mitochondria, endoplasmic reticulum and basolateral membrane [10].

Before starting the experiment, the protein concentration, measured with the Bio-Rad Kit (lyophilized bovine plasma γ-globulin as standard) was adjusted to 8 mg/ml. Vesicles used for the experiments reported in Table I, had been stored overnight on ice. Details of buffer composition are given in the figure legends.

Measurements of fluorescence quenching

The fluorescence quenching of the cyanine dye (DiS-$C_2(5)$ was measured under conditions described elsewhere [9]. The excitation and emission wavelengths were 645 and 665 nm and both the slit widths were set to 10 nm. Intra- and extra-vesicular buffers had the same ionic strength, pH, anion concentration and osmolarity (see Figure legends for experimental details). Fig. 1 shows traces superimposed without any further manipulation; each experimental condition was tested four times or more on three different membrane preparations; standard errors are shown whenever they exceeded the symbol size.

Uptake of ^3H-labeled substrate

To obtain the data shown in Table I, 5 μl of BBM vesicles suspension (250 μg protein) prepared in a buffer containing (in mM): mannitol 100, KCl 100, Hepes 20 (adjusted to pH 7.4 with Tris) were injected in 495 μl of incubation medium containing (final concentration) mannitol 100 mM, KCl 1 mM, valinomycin 2.7 μM, ethanol 0.17%, dye 3 μM, Hepes 20 mM (adjusted to pH 7.4 with Tris), proline or glucose 0.5 mM and NaCl or choline chloride 99 mM. After 5 s, the reaction was stopped by injecting into the reaction tube 3 ml of ice-cold stop solution (in mM): KCl 100, NaCl 50, Hepes 20 (adjusted to pH 7.4 with Tris)). The mixture of 3 ml stop solution plus vesicles was rapidly filtered through a millipore filter (HAWP pore size = 0.45 μm) kept under suction. The filter was washed with 3 ml of stop solution and assayed for radioactivity (Beckman LS 1801 and Ready Solv EP scintillation fluid). The nonspecific binding of the isotopes to filters was determined by measuring the uptake values at time zero.

Statistical analysis

The program Stagraphics (STSC, Rockville, MD), running on a M-28 personal computer (Olivetti, Ivrea, Italy), was used to fit equations to data (and to draw figures). The nonlinear regression subroutine calculations least-squares estimates of the parameters; the algorithm used was developed by Marquardt [11] and is a compromise between using a straight linearization method and the method of steepest descent.

Results and Discussion

Estimation of the initial rate of Na^+/proline cotransport

In a preceding paper from our laboratory, it has been shown that the fluorescence quenching of the voltage-sensitive dye DiS-$C_2(5)$ is a linear function of the membrane potential which can be created with a proper K^+ gradient in the presence of valinomycin [9]. Moreover, in that paper, a new experimental approach was described which makes it possible to measure a substrate-dependent Na^+ influx by monitoring the decay of a preset inside-negative membrane potential, in the presence of an inwardly directed Na^+ gradient [9]; Fig. 1 provides an example of this method. When BBM vesicles, prepared in a buffer containing 100 mM KCl, were injected into a cuvette buffer with similar composition (plus valinomycin and the dye), trace a of Fig. 1 was obtained; the observed fluorescence quenching was dependent on the amount of protein used and was the result of the dye redistribution across and within the membrane [12]. On the other hand, when vesicles were injected into a buffer containing KCl 1 mM + choline chloride 99 mM ($[K^+]_{in} > [K^+]_{out}$), an inside-negative membrane potential was created leading to a corresponding fluorescence quenching (Fig. 1, trace b) which was then slowly dissipated; when a Na^+ gradient (in-

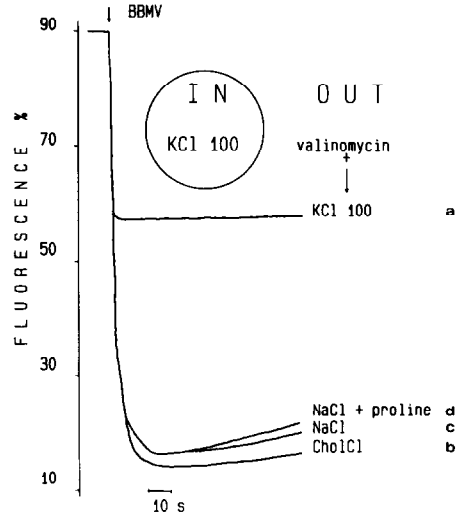

Fig. 1. Dissipation of an inside-negative membrane potential in the presence of Na^+ gradient (out > in) and L-proline. Vesicles were prepared in a buffer containing (in mM): mannitol 100, Hepes 20 (adjusted to pH 7.4 with Tris), KCl 100. 20 μl of vesicle suspension were injected into a cuvette buffer containing (final concentration): mannitol 100 mM, Hepes 20 mM (adjusted to pH 7.4 with Tris), valinomycin 2.7 μM, dye 3 μM, ethanol 1% and (in mM): (a) KCl 100 (control); (b) KCl 1, choline chloride 99; (c) KCl 1, NaCl 99; (d) KCl 1, NaCl 99, proline 0.14.

wardly directed) was present (trace c), the fluorescence quenching was dissipated more rapidly. Finally, when in the extravesicular medium both Na^+ ions and proline were present, the rate of decay of the inside-negative membrane potential was even higher and dependent on the Na^+-cosubstrate concentration (trace d). Therefore the activity of the Na^+-dependent proline transport system can be evaluated by measuring the fluorescence decay in the presence of proline and Na^+ minus the decay observed in the presence of Na^+ (trace d minus trace c).

Before using rates of fluorescence quenching decay to study kinetics of proline/Na^+ cotransport (the goal of this paper), it was important to clarify whether or not the variation of membrane potential (the recorded parameter) was itself affecting the rate of cotransport. To answer this question, in Fig. 2, the dependence of initial rate of membrane potential decay (specifically induced by proline-dependent Na^+ influx) on increasing values (at time zero) of the inside-negative membrane potential was studied. Fig. 2 shows that the Na^+/proline cotransport rate was accelerated by an inside-negative membrane potential only up to $\log([K^+]_{in}/[K^+]_{out}) = 1.5$. Under the experimental conditions of trace d of Fig. 1, when vesicles were injected into the cuvette, the membrane potential assumed the same value of the rightmost point in Fig. 2; only after a dissipation greater than 10% of the initial membrane potential, did the Na^+/proline cotransport rate begin to decrease. Therefore the initial decay of fluorescence quenching, extrapolated by traces of Fig. 1, can be used to estimate a substrate-dependent Na^+ influx which is not yet affected by the simultaneous change of membrane potential.

The 'saturation' of proline/Na^+ cotransport rate on membrane potential observed in Fig. 2 was a specific

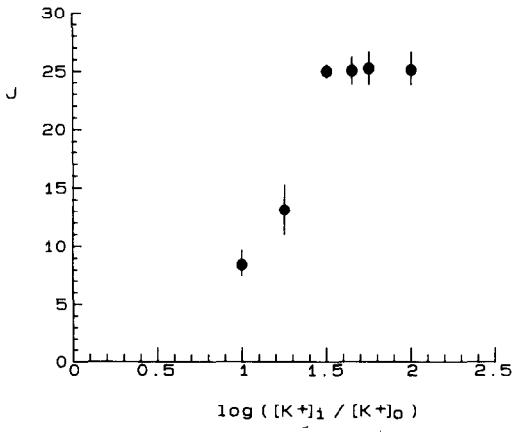

Fig. 2. Dependence of the initial rate of Na^+/proline cotransport upon the increasing inside negative membrane potential. Vesicles were prepared in a buffer containing (in mM): choline Cl 50, KCl 100, Hepes 20 (adjusted to pH 7.4 with Tris); after addition of vesicles the final incubation mixture composition was: Hepes 20 mM (adjusted to pH 7.4 with Tris), valinomycin 2.7 μM, dye 3 μM, ethanol 1% and (in mM): proline 10, NaCl 99, increasing KCl concentration (from 1 to 18) compensated by decreasing choline chloride concentrations. The initial rates of membrane potential decay induced by the proline-dependent Na^+ influx, obtained (for example) as d minus c of Fig. 1, were plotted versus the logarithmic ratio of K^+ concentration in the intra- and extra-vesicular media.

phenomenon since, as already shown elsewhere [9], the initial intravesicular depolarization (i.e., the lowest fluorescence value of trace b in Fig. 1) and the initial rate of Na^+ influx in the absence of a cosubstrate (i.e., the initial rate of membrane potential decay of trace c in Fig. 1) both linearly depended on $\log([K^+]_{in}/[K^+]_{out})$ (i.e., on increasing inside-negative membrane potentials).

Stoichiometry of proline/Na^+ and glucose/Na^+ cotransports in eel intestinal BBM vesicles

The number of possible mechanisms for proline/Na^+ cotransport is four if 1 Na^+ is cotransported with

TABLE I

Stoichiometric ratios of Na^+/glucose and Na^+/proline cotransports in brush-border membrane vesicles from the eel intestine

On the same vesicle preparation, Na^+-dependent glucose (0.5 mM) uptake, Na^+-dependent proline (0.5 mM) uptake, glucose-dependent Na^+ influx and proline-dependent Na^+ influx were measured. Uptake values of ^3H-labeled substrate were obtained as (uptake in the presence of NaCl) minus (uptake in the presence of choline chloride); experimental conditions are described in Materials and Methods. Na^+ influx values in $\Delta F\% \cdot (\text{mg protein})^{-1} \cdot \text{min}^{-1}$ were obtained as described in Fig. 1; Na^+ influx values in $\text{nmol} \cdot (\text{mg protein})^{-1} \cdot \text{min}^{-1}$ (reported in line 3) were calculated as described in Results from the fluorescence quenching values. Each value is the mean of five replicates from a representative experiment.

	Glucose	Proline	Glucose/proline
Na^+-dependent substrate uptake $(\text{nmol} \cdot (\text{mg protein})^{-1} \cdot \text{min}^{-1})$ (radioactive tracers)	19.9 ± 0.99	6.90 ± 0.89	2.88
Substrate-dependent Na^+ influx $\Delta F\% \cdot (\text{mg protein})^{-1} \cdot \text{min}^{-1}$ (fluorescent tracers)	24.8 ± 0.94	4.30 ± 0.47	5.77
Substrate-dependent Na^+ influx $\text{nmol} \cdot (\text{mg protein})^{-1} \cdot \text{min}^{-1}$ (calculated from upper line)	39.2 ± 1.49	6.80 ± 0.74	5.77

proline, but becomes 13 if 2 Na^+ are cotransported; it is therefore useful and time-saving to determine first the stoichiometry ratio of the proline/Na^+ translocation. Under zero-trans conditions and in the presence of an inside-negative membrane potential, on the same vesicle preparation, we measured: (1) the Na^+-dependent [^{3}H]glucose and [^{3}H]proline uptakes (5 s) and (2) the substrate-dependent Na^+ influx, by the fluorescence quenching technique above described; the results are reported in Table I. The Na^+-dependent [^{3}H]glucose uptake was 2.88-times higher than that of [^{3}H]proline, while the glucose-dependent Na^+ influx (estimated by the fluorescence quenching technique) was 5.77-times higher than the proline-dependent Na^+ influx. It can be concluded therefore that the glucose-dependent Na^+ influx was double the proline-dependent Na^+ influx. This calculation can be summarized as follows:

$$\frac{Na^+ \text{ cotransported with glucose}}{Na^+ \text{ cotransported with proline}} =$$

$$= (\text{glucose-dependent } Na^+ \text{ flux}$$

$$/\text{proline-dependent } Na^+ \text{ flux})$$

$$\times(Na^+\text{-dependent } [^3\text{H}]\text{glucose uptake}$$

$$/Na^+\text{-dependent } [^3\text{H}]\text{proline uptake})^{-1}$$

In two other experiments (Na^+ cotransported with glucose)/(Na^+ cotransported with proline) resulted as 6.42/3.24 and 4.07/1.96. Our suggestion is that 1 and 2 Na^+ ions are, respectively, cotransported with proline and glucose because: (1) ratios of 2 and 4, respectively, are unlikely; (2) the findings reported above match other observations (Hill plot analysis) on eel BBM vesicles [7,9]. A second, more direct, piece of evidence was provided by establishing a procedure which converts the Na^+ influxes estimated as fluorescence quenching (in $\Delta F\% \cdot min^{-1}$) to values in nmol · (mg protein)$^{-1}$ · min^{-1}. This goal was reached in three steps: (1) rates of fluorescence quenching decay (the recorded parameter) were transformed in rates of membrane potential decay (in ΔmV); (2) since the membrane potential decay of, for example, Fig. 1 trace d was caused by a substrate-dependent Na^+ influx, the variation of intravesicular Na^+ concentration was calculated with the Goldman-Hodgkin-Katz constant field equation; (3) the intravesicular volume of BBM vesicles was measured and then the values were calculated in nmol · (mg protein)$^{-1}$ · min^{-1}.

(1) The first step consisted of a calibration procedure making it possible to transform fluorescence quenching values in ΔmV. Coming back to Fig. 1, trace b was obtained when vesicles loaded with 100 mM KCl were injected into a buffer containing valinomycin, 1 mM KCl and 99 mM choline chloride; under these conditions the membrane potential was described by the Nernst equation [9] and it should assume a value of 118.2 mV (inside-negative). Therefore, in order to convert values from $\Delta F\%$ to ΔmV, for each experiment a conversion factor {118.2/(fluorescence of the lowest point of trace b minus fluorescence of trace a)} can be used. This conversion factor simply states proportionality between $\Delta F\%$ and ΔmV and, although calculated from traces recorded in the absence of Na^+ ions (Fig. 1, a and b), it can be also used with those obtained in the presence of Na^+ ions (Fig. 1, c and d), because the fluorescence quenching of diS-C_2(5) is a linear function of the membrane potential [9].

(2) Under the experimental conditions of traces c and d in Fig. 1, the inside-negative membrane potential was dissipated because for each Na^+ ion entering the vesicle (diffusional pathway and Na^+/substrate cotransport system if present), one K^+ ion could flow out (via valinomycin) lowering the membrane potential [9]. The membrane potential is numerically described by the Goldman-Hodgkin-Katz constant field equation which, under the experimental conditions of Fig. 1, can be written:

$$\Delta E = \frac{RT}{F} \ln \frac{P_K[1]_o + P_{Na}[99]_o + P_{Cl}[100]_i}{P_K[K^+]_i + P_{Na}(100 - [K^+]_i) + P_{Cl}[100]_o} \quad (1)$$

where the intravesicular Na^+ concentration was (100 − $[K^+]_i$) for the reason considered above. By using Eqn. 1, we calculated and plotted in Fig. 3 the dependence of membrane potential on intravesicular K^+ concentration ($[K^+]_i$) ranging from 100 to 80 mM, assigning to P (permeability coefficients) four sets of reasonable values (reported in the legend). For example when vesicles were injected in the cuvette, under the experimental conditions of trace c in Fig. 1 (Na^+ gradient, no Na^+-cosubstrate), the membrane potential difference should assume the rightmost value of line a of Fig. 3; for this simulation we used the permeability coefficients, rela-

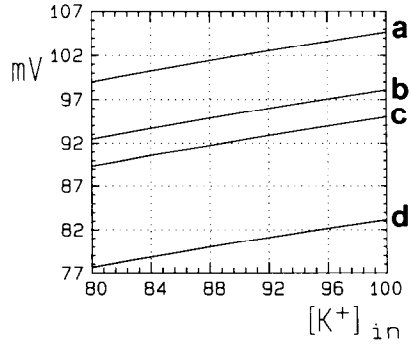

Fig. 3. Theoretical dependence of membrane potential on intravesicular K^+ and Na^+ concentrations. Membrane potential values were calculated with the Goldman-Hodgkin-Katz equation, as reported in Results, using the following permeability coefficients, relative to $P_{gluconate} = 1$: (a) $P_K = 1000$ (valinomycin), $P_{Na} = 5$, $P_{Cl} = 2$ [10]; (b) $P_K = 1000$, $P_{Na} = 10$, $P_{Cl} = 2$; (c) $P_K = 1000$, $P_{Na} = 5$, $P_{Cl} = 10$; (d) $P_K = 500$, $P_{Na} = 5$, $P_{Cl} = 10$.

tive to $P_{gluconate} = 1$, estimated for eel intestinal BBM vesicles: $P_K = 1000$ (valinomycin), $P_{Na} = 5$, $P_{Cl} = 2$ [9]. Moreover, in the presence of both Na^+- and proline gradients (Fig. 1 trace d), the viability of Na^+/proline carrier should increase Na^+ permeability; for this reason the line b of Fig. 3 was calculated with a P_{Na} value higher than line a. Surprisingly, within the range of intravesicular K^+ concentrations 100–80 mM (corresponding to Na^+ concentrations 0–20 mM) the lines of Fig. 3 were practically parallel. This finding indicated that the variation of membrane potential (ΔmV) was determined by the intravesicular K^+ concentration independently (with variables and parameters of Eqn. 1 assuming the values of Fig. 3) from the permeability coefficient used and from the absolute starting mV values. Therefore, we could use Fig. 3 as a calibration plot, in order to obtain from the ΔmV values (see step 1) the variation of the intravesicular Na^+ concentration.

(3) Finally from the distribution of D-[^{3}H]glucose in the intravesicular volume after 120 min of incubation (equilibrium value, data not shown) the volume of BBM vesicles, from eel intestinal mucosa resulted as 1.15 ± 0.14 μl/mg protein. (A value of 1 μl/mg protein has been suggested elsewhere for BBM vesicles prepared from the rabbit kidney [13]).

With this procedure, the values of glucose-dependent and proline-dependent Na^+ influx in nmol · (mg protein)$^{-1}$ · min^{-1} were calculated and, for a representative experiment, are reported in Table I (third row of data). The same conclusion was reached in two other experiments. These results lead us to conclude that 1 and 2 Na^+ ions are cotransported with each proline and glucose molecule, respectively.

Dependence of proline / Na^+ cotransport on extravesicular Na^+ concentration

The dependence of the rate of Na^+/proline cotransport on the extravesicular Na^+ concentration can be described by the Hill equation

$$J = J_{max} \cdot [Na^+]^n / (K_{Na}^n + [Na^+]^n) \quad (2)$$

where J_{max} = maximal rate, $K_{Na} = Na^+$ concentration giving half-maximal rate, n = Hill index or 'the number of substrate binding sites per molecule of enzyme' (see Refs. 14 and 15 for the limits of this procedure).

With the fluorescence quenching technique described above, the dependence of Na^+/proline cotransport rate upon Na^+ concentration in the extravesicular medium was studied and the results from a representative experiment are reported in Fig. 4 according to Woolf-Augustinsson-Hofstee [14]; the plot-fitting data should be linear when $a = 1$ and curved when $n > 1$. Visual inspection of Fig. 4 suggests a linear behavior.

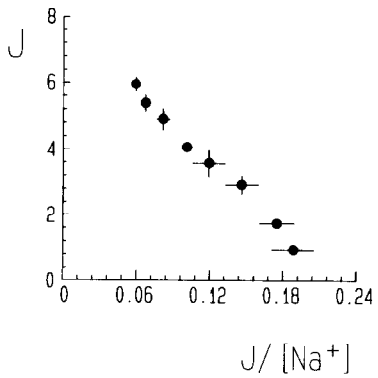

Fig. 4. Dependence of the initial rate of proline/Na^+ cotransport on extravesicular Na^+ concentration, in brush-border membrane vesicles from the eel intestine. The data were plotted according to Woolf-Augustinsson-Hofstee [14]; the three parameters of Eqn. 2 (J_{max}, n and K_{Na}) were estimated with a nonlinear regression subroutine; n resulted as ($\pm$S.E. over the estimated parameter) 0.934 ± 0.177. Vesicles were prepared in a buffer containing (in mM): mannitol 100, Hepes 20 (adjusted to pH 7.4 with Tris), KCl 100, 20 μl of the vesicle suspension were injected into a similar buffer containing in addition valinomycin 2.7 μM, ethanol 1%, dye 3 μM, and (in mM) L-proline 0.3, KCl 1, increasing NaCl concentration (from 5 to 99) compensated by decreasing choline chloride concentrations.

Furthermore, the three parameters of Eqn. 2 (J_{max}, n and K_{Na}) were estimated with a nonlinear regression subroutine; over two experiments, n resulted as ($\pm$S.E. over the estimated parameter) 0.934 ± 0.177 (data of Fig. 4) and 0.867 ± 0.363. (In another set of experiments, under identical experimental conditions, an n value > 1 for Na^+/glucose cotransport was obtained [9]).

Kinetics of Na^+/proline cotransport in eel intestinal BBM vesicles

The dependence of the initial rate of Na^+/proline cotransport on both proline and Na^+ concentrations was measured, in BBM vesicles from the eel intestine. Results are reported in Figs. 5 and 6 in a Lineweaver-Burk fashion; the lines interpolating rate values were obtained with a program of unweighted linear regression.

Possible mechanisms of the bireactant system under investigation are: (1) ordered with $proline_{out}$ binding prior to Na_{out}; (2) ordered with Na_{out} binding prior to $proline_{out}$; (3) random; (4) ping-pong. The theoretical work of Segel [14] provided the frame to fit the data into (Table II), assuming that the carrier cannot translocate: (1) Na^+ without proline (which is impossible to demonstrate lacking a specific inhibitor of proline/Na^+ cotransport); (2) proline without Na^+ [5]. Visual inspection of Fig. 5 suggests that the family of lines had no common intercept on the $1/v$ = axis while in Fig. 6, the interpolating lines tended to intersect on the $1/v$-axis. These findings exclude the possibility of a ping-pong

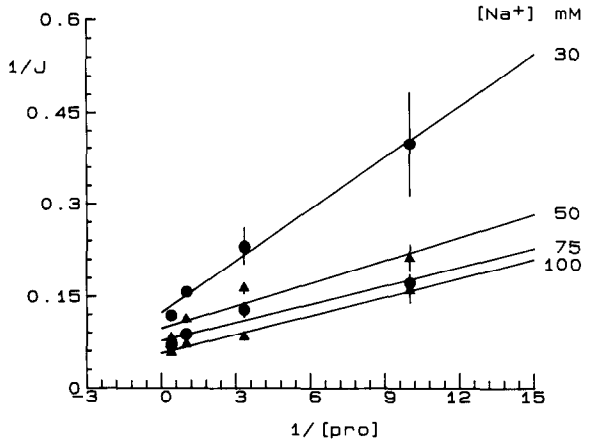

Fig. 5. Dependence of initial rate of proline/Na^+ cotransport on extravesicular proline concentration, in brush-border membrane vesicles from the eel intestine. Data were plotted according to Lineweaver-Burk; rates were estimated by the fluorescence quenching technique and J values were expressed in $\Delta F\% \cdot (\text{mg protein})^{-1} \cdot \text{min}^{-1}$. Vesicles were prepared in a buffer containing (in mM): mannitol 100, Hepes 20 (adjusted to pH 7.4 with Tris), KCl 100. 20 μl of the vesicle suspension were injected into a similar buffer containing: mannitol 100 mM, KCl 1 mM, valinomycin 2.7 μM, ethanol 1%, dye 3 μM, Hepes 20 mM (adjusted to pH 7.4 with Tris), increasing NaCl concentration (from 30 to 100 mM) compensated by decreasing choline chloride concentration, and L-proline concentration ranging from 0.1 to 2.5 mM.

mechanism, because the families of interpolating lines should result parallel in both Lineweaver-Burk plots.

Moreover Figs. 5 and 6 suggest to exclude the following mechanisms: (1) random, since the same pattern should have been found in both plots (see Table II); (2) ordered Na^+/proline, because lines should have been convergent on $1/y$-axis in Fig. 5 and not in Fig. 6, as observed. On the other hand it must be stressed the obvious that the experimental error (shown by bars) of data reported in Figs. 5 and 6, affected also the value of the intercept on $1/v$-axis making very difficult to establish, in any plot, where exactly the family of lines was intersecting. For these reasons, further support to proline/Na^+ ordered mechanism was seeked by fitting rate equations to the data.

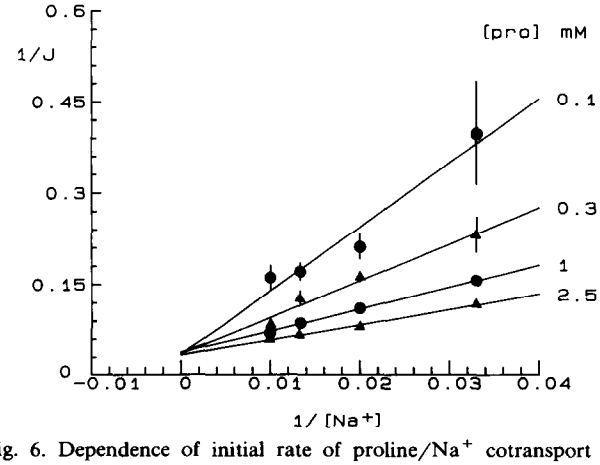

Fig. 6. Dependence of initial rate of proline/Na^+ cotransport on extravesicular Na^+ concentration, in brush-border membrane vesicles from the eel intestine. Experimental conditions are reported in the legend to Fig. 5.

TABLE II

Possible behaviors of Lineweaver-Burk plots for the proline/Na^+ cotransport (adapted from Ref. 14)

C (competitive) = the family of reciprocal plots intersect on the $1/v$-axis and above the horizontal axis. U (uncompetitive) = the family of reciprocal plots parallel with positive slopes. NC (noncompetitive) = the family of reciprocal plots intersect on the horizontal axis and to the left of the $1/v$-axis. MT (mixed type) = the family of reciprocal plots intersect above or below the horizontal axis and to the left of the $1/v$-axis. α is a coefficient present in the rate-equation of the random mechanism.

	$1/v$ versus 1/[proline] (increasing [Na^+])	$1/v$ versus [Na^+] (increasing [proline])
Ordered proline/Na^+	MT	C
Ordered Na^+/proline	C	MT
Random ($\alpha = 1$)	NC	NC
Random ($\alpha < > 1$)	MT	MT
Ping-pong	U	U

Fitting rate equations to experimental data

Assuming that all binding and dissociation steps were very rapid compared to the translocation through the membrane (rapid equilibrium assumptions), the following equations describing the activity of a bireactant system, were obtained by Segel [14].

Rapid equilibrium ordered proline/Na^+ mechanism (Eqn. VI-59 in Ref. 14):

$$J = \{J_{max} \cdot [Na^+] \cdot [\text{proline}]\} \times \{(K_{Na} \cdot K_{pro}) + (K_{Na} \cdot [\text{proline}]) + ([Na^+] \cdot [\text{proline}])\}^{-1} \quad (3)$$

where J_{max} is the maximal rate, K_{Na} and K_{pro} are the dissociation constants for the complex enzyme-substrate.

Rapid equilibrium ordered Na^+/proline mechanism (Eqn. VI-59 in Ref. 14):

$$J = \frac{J_{max} \cdot [Na^+] \cdot [\text{proline}]}{(K_{Na} \cdot K_{pro}) + (K_{pro} \cdot [Na^+]) + ([Na^+] \cdot [\text{proline}])} \quad (4)$$

Rapid equilibrium random Na^+/proline mechanism (Eqn. VI-2 in Ref. 14):

$$J = \{J_{max} \cdot [\text{proline}] \cdot [Na^+]\} \{(\alpha K_{pro} \cdot K_{na}) + (\alpha K_{pro} \cdot [Na^+]) + (\alpha K_{Na} \cdot [\text{proline}]) + ([\text{proline}] \cdot [Na^+])\}^{-1} \quad (5)$$

where only Na^+ and proline extravesicular concentrations are considered and, if the two substrates bind

TABLE III

Fitting model Eqns. 3–5 of a bireactant system to rates of proline/Na^+ cotransport in brush-border membrane vesicles from the eel intestine

Results from three experiments on different membrane preparations are shown. SS = sum of least squares; df = degrees of freedom. Values of the estimated parameter ± standard error are reported. Units were: $\Delta F\% \cdot (\text{mg protein})^{-1} \cdot \text{min}^{-1}$ for J_{max}; mM for K_{Na} and K_{pro}.

Mechanism	SS(df)	J_{max}	K_{Na}	K_{pro}	α
1 Ordered pro/Na^+	110 (61)	28.3 ± 3.2	65.5 ± 15.5	0.41 ± 0.07	
Ordered Na^+/pro	278 (61)	15.0 ± 1.1	2575 ± 13203	0.007 ± 0.038	
Random	111 (60)	29.3 ± 4.6	717 ± 2299	0.35 ± 0.15	0.10 ± 0.34
2 Ordered pro/Na^+	143 (61)	14.4 ± 1.2	24.1 ± 7.5	0.25 ± 0.08	
Ordered Na^+/Pro	204 (61)	10.5 ± 0.4	2250 ± 29447	0.002 ± 0.029	
Random	144 (60)	14.5 ± 1.6	951 ± 6698	0.23 ± 0.16	0.03 ± 0.19
3 Ordered pro/Na^+	72 (61)	26 ± 10	153 ± 88	0.34 ± 0.10	
Ordered Na^+/pro	108 (61)	11.6 ± 1.7	10398 ± 327229	0.004 ± 0.115	
Random	72 (60)	38.8 ± 38.0	215 ± 521	0.215 ± 0.199	1.20 ± 4.29

randomly, the binding of one substrate changes the dissociation constant for the other substrate by a factor α.

These three equations were fitted to the initial rate values in order to evaluate: (1) the equation best fitting the data; (2) to calculate the values for kinetic parameters. Table III reports the sum of the least squares (SS), degrees of freedom (df) and the estimated parameters ± standard error (S.E.), for three experiments. Since a robust non-linear regression program will always find values for parameters present in any equation, the critical point is to fix a number of criterions to establish the equation best fitting the data. To reach this goal we considered the sum of least squares (SS) and the standard error (S.E.) over the estimated parameters.

As stated elsewhere "comparing models with the same number of parameters is easy: the fit with the lower sum of squares is superior, for its curve lies closer to the points. The statistical significance is obtained by

$$F = SS_1/SS_2 \tag{6}$$

where both numerator and denominator have N–V degrees of freedom (SS = residual sum of squares of each fit, N = number of data points; V = number of parameters fit by the program). Comparing two models with a different number of parameters (as Eqn. 3 (three parameters) and Eqn. 5 (four parameters to be estimated)) is less straightforward, because increasing the number of parameters gives more flexibility to the curve-fitting procedure, and almost always leads to a curve that is closer to the points. The question is whether the improved fit is worth the cost (in lost degrees of freedom) of the additional parameter or parameters. This question is usually answered statistically by performing an F test with the following equation:

$$F = \frac{(SS_1 - SS_2)/(df_1 - df_2)}{SS_2/df_2} \tag{7}$$

Here SS refers to the sum of squares, and df refers to the number of degrees of freedom (number of data points minus the number of parameters). The subscript 1 refers to the fit with fewer parameters, the more simple model. A P value is obtained from the F value by consulting a standard table [16] using $(df_1 - df_2)$ and df_2 degrees of freedom. A small P value indicates that the more complex model (with more parameters) fits the data significantly better than the simple model." [17].

Table III shows that the lowest sum of least squares (SS) was obtained by fitting Eqn. 3 (ordered proline /Na^+) to rate values; in order to answer the question whether or not the lower sum of squares (SS) values were statistically significant, the F test was used and the results are shown in Table IV. In other words, Table IV answers the following question: does the mechanism, indicated on the left, fit the data better than the ordered Na^+/proline (first column) or random (second column) mechanisms?

TABLE IV

Statistical significance (F test) of the comparison between the SS (sum of squares) resulting from different model equations

The table answers the question: does (for example) the equation of ordered proline/Na^+ mechanism, fit the data better than (for example) the equation of ordered Na^+/proline mechanism? The F test was performed using Eqns. 6 and 7 (reported in Results) and the SS and df values of Table III.

	Ordered Na^+/proline	Random	Experiment
Ordered proline/Na^+	yes ($0.01 > P$)	no ($P > 0.05$)	1
	no ($P > 0.05$)	no ($P > 0.05$)	2
	yes ($0.05 = P$)	no ($P > 0.05$)	3
Random	yes ($0.01 > P$)		1
	yes ($0.01 > P$)		2
	yes ($0.01 > P$)		3

Table IV shows that: (a) the ordered proline/Na^+ (2 times over 3) and the random (3 over 3) mechanisms fitted the data significantly better than the ordered Na^+/proline one; (b) in all the other cases the sum of squares (SS) were not statistically different. These considerations excluded the ordered Na^+/proline mechanism, but could not lead us to prefer any of the remaining two.

Fortunately, the data reported in Table III can be used as a base for other considerations. It has been stressed elsewhere [17] that non-linear regression procedures provide families of possible solutions within the range estimated parameter ± standard error. Therefore, as already suggested by Cleland [18], the standard error values provided by the computer-program with the estimated parameter "are quite useful as an informal measured of the goodness of a fit" [17]. In Table III, fitting Eqn. 4 (ordered Na^+/proline mechanism) to data always led to: (a) solutions unlikely high for K_{Na} and low for K_{pro}; (b) enormous standard errors over the estimated parameters. Moreover, by fitting Eqn. 4 (random mechanism), the lower sum of least squares could be reached only: (1) when solutions were unlikely high for K_{Na} (2 times over 3); (2) when estimates of K_{Na} were characterized by a very large standard error. These findings indicate that Eqn. 3 (ordered proline/Na^+ mechanism) fits the data better than Eqn. 5 (random mechanism).

To sum up, in eel intestinal BBM vesicles, the proline/Na^+ cotransport does not take place via a ping-pong mechanism, as indicated by graphical evidence of Figs. 5 and 6. Further conclusions were reached by fitting rate equations to the data. The ordered Na^+/proline mechanism was excluded because: (1) the sum of least squares was always significantly higher (Tables III and IV) than those obtained for the remaining mechanisms; (2) it was not possible to determine carefully the kinetic parameters. Finally the random mechanism could be ruled out, since the estimate for the K_{Na} parameters was always characterized by a very large standard error (Table III).

These considerations, taken together, suggest that the Eqn. 3, describing an ordered mechanism with $proline_{out}$ binding to the cotransporter prior to Na_{out}, is the one best fitting the experimental data.

Conclusions

Fig. 1 shows how the dissipation of an inside-negative membrane potential (monitored with a voltage-sensitive fluorescent dye) can be used to estimate a substrate-dependent Na^+ influx, the experimental conditions involved an inwardly directed Na^+ gradient and an inside-negative membrane potential, therefore the driving forces were oriented as it occurs in vivo [9].

In this paper, estimating the substrate-dependent Na^+ influx with a fluorescence quenching technique in BBM vesicles prepared from the intestinal mucosa of the eel, we provided evidence that 2 Na^+ are cotransported with 1 glucose; the same conclusion was unequivocally reached for the chicken intestinal BBM by Kimmich and Randles [15]. On the other hand, it has been suggested [3,4] that mammalian intestine possesses two distinct Na^+/glucose cotransporters with different stoichiometric ratios.

To obtain information on the mechanism of proline/Na^+ cotransport, a low-cost program for the personal computer has been used to fit equations to rate values; other examples can be found in Refs. 19 and 20. By the graphical analysis of the rate values usually used (Lineweaver-Burk plot and so on) only two of the parameters present in a rate equation, can be simultaneously estimated; the remaining parameters are then calculated using replots of the slopes or intercepts, previously obtained, sometimes ignoring their standard errors. On the other hand, non-linear regression programs: (1) fit directly the model rate-equation to the data; (2) estimate all parameters; (3) provide a number of indications on the goodness of the performed fit. At the moment, we believe, the use of non-linear regression programs is not generalized because the reader of scientific papers is not helped, by the authors, to understand the cryptic description of what is going on.

In this paper we provide evidence that 1 Na^+ is cotransported with 1 proline (Fig. 4); moreover, we show that proline/Na^+ cotransport, in BBM vesicles from the eel intestine, follows an ordered mechanism with $proline_{out}$ binding prior to Na_{out} (Figs. 5 and 6); rates were measured under zero-trans conditions, in the presence of an inside-negative membrane potential. As model explaining measured rates, only equations obtained under rapid equilibrium assumptions were used; the interested reader will find elsewhere [3] a point of view, different from ours, about choosing between rapid equilibrium and steady-state assumptions.

On the other hand, the proline/Na^+ cotransport, occurring on IMINO carrier, of the intestinal BBM vesicles in the rabbit "can be described as a rapid equilibrium iso-ordered ter-ter system, where two sodium ions first combine with the carrier to increase its affinity for proline" [8]. The discrepancy between our and the other study could be possibly explained by technical differences: (a) BBM vesicles were, respectively, freshly prepared and stored in liquid nitrogen; (b) experimental conditions involved, respectively, inside-negative and short-circuited membrane potential; (c) experimental conditions emphasized errors, respectively, at low Na^+-concentration (fluorescent tracers, our case) and high proline concentration (radioactive tracers, the other case). However, we prefer to believe that proline/Na^+ cotransporters are different in eel

and rabbit, basing our statement also on the different inhibition pattern shown by alanine and phenylalanine on [^{3}H]proline uptake [5,6,21].

Future studies are needed to characterize the eel proline/Na^+ cotransporter in order to understand the molecular base of such a difference in mammals.

Acknowledgements

This work was supported by a grant (40%) from Ministero della Pubblica Istruzione. We are grateful to Prof. Raimondo Anni (Dipartimento di Fisica, Lecce) and to Prof. Giorgio Semenza (ETH, Zürich) for stimulating discussions.

References

1 Crane, R.K. (1965) Fed. Proc. 24, 1000–1005.
2 Christensen, H.N. (1985) J. Membr. Biol. 84, 97–103.
3 Hopfer, U. (1987) in Physiology of Gastrointestinal Tract (Johnson, L.R., ed.), 2nd Edn., pp. 1499–1523, Raven Press, New York.
4 Semenza, G. and Corcelli, A. (1986) in Molecular and Cellular Basis of Digestion (Desnuelle, P., ed.), Ch. 21, pp. 381–412, Elsevier, Amsterdam.
5 Vilella, S., Ahearn, G.A., Cassano, G. and Storelli, C. (1988) Am. J. Physiol. 255, R648–R653.
6 Stevens, B.R., Ross, H.J. and Wright, E.M. (1982) J. Membr. Biol. 66, 213–225.
7 Stevens, B.R., Kaunitz, J.D. and Wright, E.M. (1984) Annu. Rev. Physiol. 46, 417–431.
8 Stevens, B.R. and Wright, E.M. (1987) J. Biol. Chem. 262, 6546–6551.
9 Cassano, G., Maffia, M., Vilella, S. and Storelli, C. (1988) J. Membr. Biol. 101, 225–236.
10 Storelli, C., Vilella, S. and Cassano, G. (1986) Am. J. Physiol. 251, R463–R469.
11 Marquardt, D.W. (1963) J. Soc. Indust. Appl. Math. 11, 431–441.
12 Sims, P.J., Waggoner, A.S., Wang, C.H. and Hoffman, J.F. (1974) Biochemistry 13, 3315–3330.
13 Chen, P., Illsley, N.P. and Verkman, A.S. (1988) Am. J. Physiol. 254, F114–F120.
14 Segel, I.H. (1975) Enzyme Kinetics, John Wiley & Sons, New York.
15 Kimmich, G.A. and Randles, J. (1984) Am. J. Physiol. 247, C74–C82.
16 Spiegel, M.R. (1975) Probability and Statistics, McGraw-Hill Book Company, New York.
17 Motulsky, H.J. and Ransnas, L.A. (1987) FASEB J. 1, 365–374.
18 Cleland, W.W. (1979) in Methods in Enzymology (Purich, D.L., ed.), Vol. 63, pp. 103–139, Academic Press, New York.
19 Restrepo, D. and Kimmich, A.G. (1985) Am. J. Physiol. 248, C498–C509.
20 Robinson, J.W.L. and Van Melle, G. (1983) J. Physiol. 344, 177–187.
21 Vilella, S., Cassano, G. and Storelli, C. (1989) Biochim. Biophys. Acta 984, 188–192.